

# Strength degradation mechanism of iron coke prepared by mixed coal and Fe<sub>2</sub>O<sub>3</sub>

Yin, C., Qiu, S., Zhang, S., Sher, F., Zhang, H., Xu, J. & Wen, L.

Author post-print (accepted) deposited by Coventry University's Repository

**Original citation & hyperlink:**

Yin, C, Qiu, S, Zhang, S, Sher, F, Zhang, H, Xu, J & Wen, L 2020, 'Strength degradation mechanism of iron coke prepared by mixed coal and Fe<sub>2</sub>O<sub>3</sub>', Journal of Analytical and Applied Pyrolysis, vol. 150, 104897.

<https://dx.doi.org/10.1016/j.jaap.2020.104897>

DOI 10.1016/j.jaap.2020.104897

ISSN 0165-2370

Publisher: Elsevier

**NOTICE: this is the author's version of a work that was accepted for publication in Journal of Analytical and Applied Pyrolysis. Changes resulting from the publishing process, such as peer review, editing, corrections, structural formatting, and other quality control mechanisms may not be reflected in this document. Changes may have been made to this work since it was submitted for publication. A definitive version was subsequently published in Journal of Analytical and Applied Pyrolysis, 150, (2020) DOI: 10.1016/j.jaap.2020.104897**

© 2020, Elsevier. Licensed under the Creative Commons Attribution-NonCommercial-NoDerivatives 4.0 International <http://creativecommons.org/licenses/by-nc-nd/4.0/>

Copyright © and Moral Rights are retained by the author(s) and/ or other copyright owners. A copy can be downloaded for personal non-commercial research or study, without prior permission or charge. This item cannot be reproduced or quoted extensively from without first obtaining permission in writing from the copyright holder(s). The content must not be changed in any way or sold commercially in any format or medium without the formal permission of the copyright holders.

This document is the author's post-print version, incorporating any revisions agreed during the peer-review process. Some differences between the published version and this version may remain and you are advised to consult the published version if you wish to cite from it.

# **Strength degradation mechanism of iron coke prepared by mixed coal and Fe<sub>2</sub>O<sub>3</sub>**

Chen Yin<sup>a,b</sup>, Shuxing Qiu<sup>a,d</sup>, Shengfu Zhang<sup>a,b,\*</sup>, Farooq Sher<sup>c</sup>, Hua Zhang<sup>a,b</sup>, Jian Xu<sup>a,b</sup>,

Liangying Wen<sup>a,b,\*</sup>

<sup>a</sup>College of Materials Science & Engineering, Chongqing University, Chongqing 400044, P.R. China

<sup>b</sup>Chongqing Key Laboratory of Vanadium-Titanium Metallurgy & Advanced Materials, Chongqing University, Chongqing 400044, P.R. China

<sup>c</sup>School of Mechanical, Aerospace and Automotive Engineering, Faculty of Engineering, Environment and Computing, Coventry University, Coventry CV1 5FB, UK

<sup>d</sup>State Key Laboratory of Vanadium and Titanium Resources Comprehensive Utilization, Panzhihua Iron & Steel Research Institute, Panzhihua 617000, P.R. China

Chen Yin, E-mail: [yinchen@cqu.edu.cn](mailto:yinchen@cqu.edu.cn)

Shuxing Qiu, E-mail: [qiusx105@163.com](mailto:qiusx105@163.com)

\*Shengfu Zhang (Corresponding author), E-mail: [zhangsf@cqu.edu.cn](mailto:zhangsf@cqu.edu.cn)

Farooq Sher (Corresponding author), E-mail: [Farooq.Sher@coventry.ac.uk](mailto:Farooq.Sher@coventry.ac.uk)

Hua Zhang, E-mail: [zhanghuacqu@163.com](mailto:zhanghuacqu@163.com)

Jian Xu, E-mail: [jxu@cqu.edu.cn](mailto:jxu@cqu.edu.cn)

\*Liangying Wen (Corresponding author), E-mail: [cquwen@cqu.edu.cn](mailto:cquwen@cqu.edu.cn)

## **Abstract**

Iron coke, as a new type of blast furnace burden is helpful for energy saving, emission reduction and green production of iron making. This study aims to investigate the strength degradation mechanism of iron coke prepared by mixed coal and  $\text{Fe}_2\text{O}_3$  to provide a theoretical direction to improve its strength. Coking and pyrolysis experiments of mixed coal and  $\text{Fe}_2\text{O}_3$  were carried out between 400 and 500 °C temperature. Gieseler plastometer and derivative thermogravimetric (DTG) showed that added  $\text{Fe}_2\text{O}_3$  inhibited the thermoplasticity and pyrolysis process of mixed coal during coking. X-ray diffraction (XRD) and Fourier transform infrared spectroscopy (FT-IR) results showed that added  $\text{Fe}_2\text{O}_3$  decreased the aromaticity and average stacking height, but increased the interlayer spacing of crystallite, aliphatic chain length and hydrocarbon-generating potential of mixed coal during coking. Further, gas chromatography-mass spectrometer (GC-MS) analysis suggested that the added  $\text{Fe}_2\text{O}_3$  inhibited the cleavage of  $\text{C}_{\text{al}}\text{-O}$ ,  $\text{C}_{\text{al}}\text{-S}$ ,  $\text{C}_{\text{al}}\text{-N}$ ,  $\text{C}_{\text{al}}\text{-C}_{\text{ar}}$  and  $\text{C}_{\text{al}}\text{-C}_{\text{al}}$  bonds, reduced the generation of ethylbenzene, o-xylene and unbranched alkanes with carbon atoms in 24-26, thus decreased the amount of fluid phase generated in coking and ultimately degraded the strength of iron coke.

**Keywords:** Iron coke, Strength degradation, Thermoplastic behavior, Structure transformation, Pyrolysis.

## 1. Introduction

With a rapid increase in environmental protection pressure, steel companies are eagerly looking for new technologies that are conducive for green production. Coke could be an indispensable burden for blast furnace ironmaking. Therefore, it has been studied that improving its reactivity is helpful to accelerate the indirect reduction rate of iron ore, and to increase the reaction efficiency of blast furnace, thereby realize energy saving and consumption reduction in the process of ironmaking [1, 2]. Iron, as a transition group metal, can reduce the energy barrier formed by unstable activated complexes, promote the formation of carbon-oxygen complexes, and attract CO in the carbon-oxygen complexes through the reduction of iron oxides during gasification process to accelerate the gasification [3]. In addition, as the final product of blast furnace ironmaking, iron has no adverse effect on the blast furnace. Therefore, the use of iron-based additives to improve coke reactivity has obvious advantages [4-7].

Many studies show that [8-17] iron-containing substances are harmful to the strength of iron coke while catalyzing its reactivity, especially to the index of coke strength after reaction (CSR). As a result, the role of iron coke in the blast furnace is weakened, which is not conducive to its application in the blast furnace. It is well known that the strength of coke is closely related to the behavior of the fluid phase (metaplast) during coal pyrolysis, which determines the fluidity of coal during the thermoplastic stage. At present, fluidity and swelling are commonly used to represent the thermoplasticity of coal. The better the fluidity of coal, the lower the reactivity and the higher the CSR [18]. Studies found that the fluidity of coal in thermoplastic stage has a

parabolic relationship with the coke reactivity index (CRI) and CSR, and the CRI reaches its maximum when the fluidity is around 100 ddpm, and CRI reached to a minimum value when the fluidity is around 200 ddpm, while the change of CSR is opposite [19, 20]. Khan *et al.* [21] studied the swelling and thermoplasticity changes of coal with added  $\text{Fe}_2\text{O}_3$  and  $\text{Fe}_3\text{O}_4$  and verified that iron oxides is harmful to the fluidity of coal. Moreover,  $\text{Fe}_2\text{O}_3$  has a more obvious deterioration effect on the thermoplasticity of coal than other iron minerals [21]. Through co-pyrolysis experiment of coal and  $\text{Fe}_2\text{O}_3$ , Uchida *et al.* [22] found that  $\text{Fe}_2\text{O}_3$  reduced the thermoplasticity of coal while accompanied by its own reduction. However, it is worth noting that the above studies are based on the characteristics of the fluidity change of coal in the thermoplastic stage after adding iron-containing substance. There are only a few studies on the components of fluid phase. Therefore, it is important to understand the composition and structural transformation of mixed coal with  $\text{Fe}_2\text{O}_3$  in the thermoplastic stage of coking [23-25].

In the present study, high reactivity iron coke was successfully prepared from mixed coal and  $\text{Fe}_2\text{O}_3$ , and its strength deterioration behavior was obtained. Further, through pyrolysis experiments and some chemical and physical tests, changes in the thermoplasticity and structural transformation of mixed coal during thermoplastic stage after adding  $\text{Fe}_2\text{O}_3$  were compared and analyzed. Finally, the mechanism of iron coke strength degradation was established. In fact, the experimental results have guiding significance for the development of the fabrication process of iron coke.

## 2. Experimental

### 2.1 Sample preparation

Four coals (Coal-A, Coal-B, Coal-C, and Coal-D received from a steel corporation located in Northeast of China) with 0.1-0.3 mm and 0.5-3.0 mm particle size were used in this work. The characterization data of these coal samples is described in Table 1. A standard mixed coal is composed of Coal-A (30 wt.%), Coal-B (20 wt.%), Coal-C (40 wt.%) and Coal-D (10 wt.%). In order to analyze the strength degradation mechanism of iron coke with more accurately, the mixed coal is pickled to remove minerals, and the detailed information shows in our previous work [26].  $\text{Fe}_2\text{O}_3$  is used as a catalyst with a particle size of less than 48  $\mu\text{m}$  that is chemically pure reagent. The samples of mixed coal with  $\text{Fe}_2\text{O}_3$  or without are named as CM- $\text{Fe}_2\text{O}_3$  and CM-RAW respectively, the addition amount of  $\text{Fe}_2\text{O}_3$  is 3 wt% based on coal mass [27].

**Table 1.** Basic thermochemical properties of coal samples.

Samples	Proximate analysis (wt.%)				Ultimate analysis (wt.%)					$R_0(\%)$	H/C
	$M_{\text{ad}}$	$V_{\text{daf}}$	$FC_{\text{d}}$	$A_{\text{d}}$	$C_{\text{daf}}$	$H_{\text{daf}}$	$O_{\text{daf}}$	$N_{\text{d}}$	$S_{\text{d}}$		
Coal-A	2.30	22.25	71.90	7.52	87.97	4.95	5.11	1.45	0.37	1.228	0.06
Coal-B	1.74	31.72	61.72	9.61	85.49	5.10	6.28	1.36	1.47	1.008	0.06
Coal-C	2.34	34.40	60.94	7.12	84.30	5.66	8.87	0.94	0.15	0.85	0.07
Coal-D	1.70	18.34	70.30	13.92	88.80	4.51	5.23	1.25	1.06	1.713	0.05

*M*: moisture. *V*: volatile matter. *FC*: fixed carbon. *A*: ash. ad: air dried basis. d: dried basis. daf: dried and ash-free basis.  $R_0$ : the maximum reflectance of vitrinite. H/C: the ratio of element H to C.

### 2.2 Iron coke preparation

Iron coke was prepared in a 2 kg laboratory coke oven. The sample (CM-RAW or CM- $\text{Fe}_2\text{O}_3$ ) with a particle of 0.5-3 mm and a weight of 2 kg was loaded into a coking tank together with 10% moisture and 0.85 t/m<sup>3</sup> bulk density. The details of this process have been described in our previous work [27]. After coke was quenched by nitrogen, the mechanical strength and thermal properties including the abrasion resistance index

( $M_{10}$ ), drop shatter index ( $M_{25}$ ), *CRI* and *CSR* were measured [27] to understand the effect of  $\text{Fe}_2\text{O}_3$  on coke strength degradation.

### 2.3 Thermoplasticity analysis

Gieseler plastometer (ZKJSLDD-4C) was used to observe changes in thermoplasticity of mixed coal during coking after adding  $\text{Fe}_2\text{O}_3$ . The sample (CM- $\text{Fe}_2\text{O}_3$  or CM-RAW) with a particle of 0.1-0.3 mm and weight  $5.0 \pm 0.1$  g was placed in a steel crucible fitted with four metal stirring blades at the bottom. Then the steel crucible was placed in a liquid metal bath at  $300^\circ\text{C}$ , and the temperature was raised to  $550^\circ\text{C}$  at a rate of  $3^\circ\text{C}/\text{min}$ . During this process, the metal stirring paddles were turned at a constant torque. When rotation speed reached to 1 ddpm, temperature and rotation degree were recorded every 1 min until the stirring paddle was no longer rotating (rotation speed  $<1$  ddpm). So, the Gieseler fluidity curve of samples could be obtained.

### 2.4 Thermal behavior analysis

Thermogravimetric analyzer (STA 449F3, NETZSCH) was used to analyze the changes in pyrolysis behavior of mixed coal after adding  $\text{Fe}_2\text{O}_3$ . About  $7 \pm 2$  mg sample (CM- $\text{Fe}_2\text{O}_3$  or CM-RAW) with a particle of 0.1-0.3 mm was heated from room temperature to  $1050^\circ\text{C}$  at a heating rate of  $10^\circ\text{C}/\text{min}$  under high purity of nitrogen gas with a flow rate of 50 mL/min. Thus, the change of samples weight with temperature was obtained, further the derivative thermogravimetric (DTG) curve of samples was derived.

### 2.5 Pyrolysis experiment

In order to study the changes in thermoplasticity and structure of mixed coal at thermoplastic stage after adding  $\text{Fe}_2\text{O}_3$ , pyrolysis experiments with different target

temperature were carried out. About 50 g sample (CM-Fe<sub>2</sub>O<sub>3</sub> or CM-RAW) with a particle of 0.1-0.3 mm was put into a corundum crucible and heated from 25°C to the target temperature (400, 425, 450, 475, and 500°C) at 10°C/min under the protection of high-purity nitrogen. These target temperatures are considered to cover the temperature range of the coal thermoplastic stage [26]. Finally, the heated mixed coal was quenched to room temperature by nitrogen to obtain the required samples.

## 2.6 XRD analysis

The changes in carbon structure of mixed coal during thermoplastic stage after adding Fe<sub>2</sub>O<sub>3</sub> were analyzed by X-ray diffractometer (MAX2500PC X, Nippon koji co. LTD). All samples were pulverized in the laboratory and screened to below 0.074 mm. The X-ray source was generated by copper *K*α radiation (40 kV, 150 mA). The scanning angular started from 15° to 90° at a rate of 4°/min, 0.02°/step. Gaussian fitting is performed on the obtained XRD spectra to obtain the required information about γ-band and π-band (002), thereby calculating the parameter  $f_a$  represents the aromaticity of mixed coal [28]. Furthermore, parameter  $d_{002}$ , and  $L_c$  represent the coal graphitization and the coal average stacking height respectively, were calculated using full width at half maximum (FWHM) and scattering angle of π-band (002) [29, 30].

## 2.7 FT-IR analysis

Fourier transform infrared spectroscopy (Nicolet iS5-FTIR, Thermo Fisher Scientific) was used to analyze the changes in structure transformation of functional groups of mixed coal during thermoplastic stage after adding Fe<sub>2</sub>O<sub>3</sub>. The sample was placed on a KBr sheet and dried under vacuum at room temperature. Each spectrum segment was scanned 32 times with a resolution of 4 cm<sup>-1</sup> and the scanning wave number range was 4000-650 cm<sup>-1</sup>. In addition, two characteristic parameters of CH<sub>2</sub>/CH<sub>3</sub> and *A-factor* reflecting the aliphatic chain length and hydrocarbon-generating



potential of coal respectively, could be obtained by fitting the curves of two regions (3000-2800  $\text{cm}^{-1}$  and 1700-1500  $\text{cm}^{-1}$ ) [26].

## 2.8 GC-MS analysis

Gas chromatography mass spectrometer (QP2010Ultra, Shimadzu) was used to analyze changes of fluid phase transformation of mixed coal during thermoplastic stage after adding  $\text{Fe}_2\text{O}_3$ . The GC-MS characteristics were described in previous studies [31] and the fluid phase can be obtained from two-step solvent extraction (first acetone, then THF) [26]. Firstly, the sample from the pyrolysis experiment were placed in acetone, and the collected extracts were named as 400-light, 425-light, 450-light, 475-light and 500-light, respectively. Then the sample was removed from acetone to THF, and the extracts collected were named as 400-heavy, 425-heavy, 450-heavy, 475-heavy and 500-heavy, respectively. Finally, the light/heavy extracts were equally divided into four parts, three of which were placed in an oven and evaporated to obtain the extract content by subtraction. The other part was refrigerated in vacuum until further analysis.

## 3. Results and discussion

### 3.1 Strength degradation of iron coke prepared by mixed coal and $\text{Fe}_2\text{O}_3$

As can be seen from Fig. 1,  $\text{Fe}_2\text{O}_3$  can significantly improve the reactivity of coke with  $\text{CO}_2$ , but its degradation effect on coke strength is also very obvious. After adding  $\text{Fe}_2\text{O}_3$ , the CRI of coke increased from 36.36% to 41.57%. And the index of  $M_{10}$  and  $M_{25}$  changed from 4.94% and 94.15% to 5.78% and 92.98% respectively when  $\text{Fe}_2\text{O}_3$  was added, which indicated that the added  $\text{Fe}_2\text{O}_3$  would degrade the abrasion resistance index and also drop shatter index of coke. The deterioration was more obvious in the

coke strength after reaction (*CSR*). The addition of  $\text{Fe}_2\text{O}_3$  reduced *CSR* from 61.94% to 42.78%. These results are consistent with the previous studies [8-17].

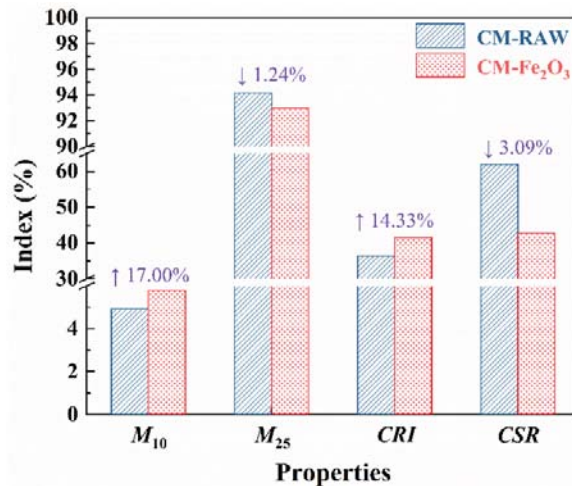


Fig. 1. Changes in coke properties after adding  $\text{Fe}_2\text{O}_3$ .

### 3.2 Changes in the thermoplasticity of mixed coal after adding $\text{Fe}_2\text{O}_3$

As shown in Fig. 2, the CM-RAW begin to soften at 422°C and then the fluidity increased with increasing temperature resulting in maximum fluidity of 195 ddpm at 455°C, after which the fluidity decreased with increasing temperature and solidified again at 491°C. The curve is convex with a thermoplastic range of 69°C. The physical changes of mixed coal during thermoplastic stage depend on the chemical changes in its molecular structure, involving the rearrangement of carbon molecules to form a fluid phase and solidification of fluid phase into low temperature graphitized carbon material (semi-coke) [32]. The thermoplastic characteristics of CM- $\text{Fe}_2\text{O}_3$  are similar to those of CM-RAW. Its softening temperature is 4°C higher than CM-RAW, and the solidification temperature is 2°C lower than CM-RAW. Moreover, the maximum fluidity and thermoplastic range of CM- $\text{Fe}_2\text{O}_3$  were reduced by 40 ddpm and 6°C compared with CM-RAW, respectively. Despite the dilution effect of  $\text{Fe}_2\text{O}_3$  on thermoplasticity of

mixed coal, the actual plasticity range and maximum fluidity value of CM-Fe<sub>2</sub>O<sub>3</sub> may be slightly larger than the measured value. However, the dilution effect of Fe<sub>2</sub>O<sub>3</sub> is negligible because Fe<sub>2</sub>O<sub>3</sub> is added in a small amount (3%), and the volume of two samples in the crucible does not change significantly. Therefore, the added Fe<sub>2</sub>O<sub>3</sub> will reduce the thermoplasticity of coal during coking.

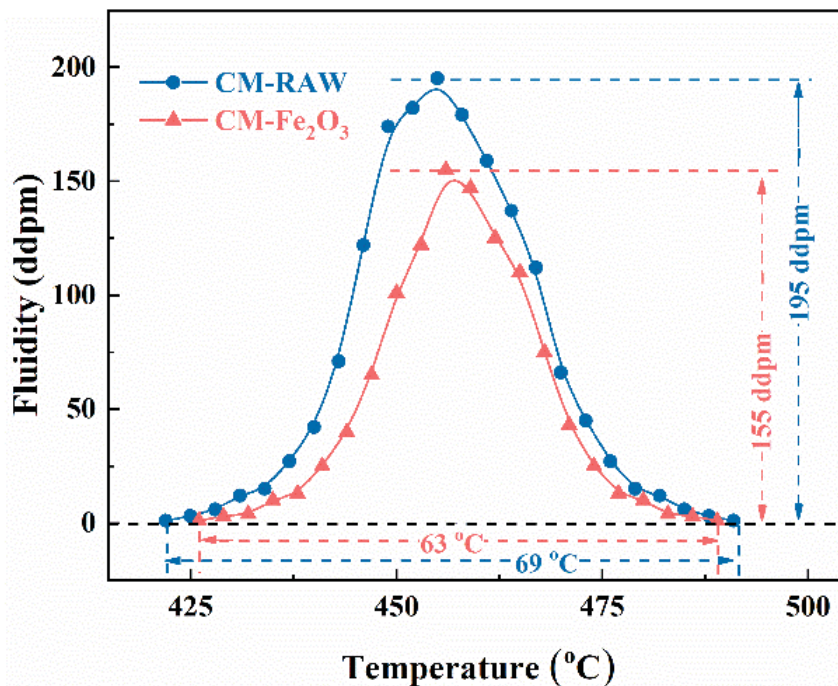


Fig. 2. Gieseler fluidity curves of mixed coal samples.

### 3.3. Changes in the pyrolysis behavior of mixed coal after adding Fe<sub>2</sub>O<sub>3</sub>

Fig. 3 provides DTG curves of mixed coal. According to Fig. 3(a), the maximum weight loss rate of CM-RAW corresponds to a temperature of 471°C, which is close to the temperature of maximum fluidity. The maximum weight loss rate of CM-Fe<sub>2</sub>O<sub>3</sub> is 0.137% min<sup>-1</sup>, which is 0.002% min<sup>-1</sup> less than CM-RAW. The results also show that the Fe<sub>2</sub>O<sub>3</sub> added inhibits the pyrolysis process of mixed coal during thermoplastic stage.

According to the order of covalent bond breaking, the coking process is divided

into multiple stages as shown in Table 2 [33-42]. The peak-differentiating and imitating of DTG curve is performed to obtain the relevant information about the above bonds. It can be seen that after addition of  $\text{Fe}_2\text{O}_3$ , the content of first type bond ( $\text{C}_{\text{al-O}}$ ,  $\text{C}_{\text{al-S}}$ , and  $\text{C}_{\text{al-N}}$ ) decreased by 0.01, the content of second type bond ( $\text{C}_{\text{al-C}_{\text{al}}}$ ) decreased by 0.94, and the content of third type bond ( $\text{C}_{\text{al-C}_{\text{ar}}}$ ) decreased by 0.13. It indicated that the added  $\text{Fe}_2\text{O}_3$  inhibits the breaking of  $\text{C}_{\text{al-C}_{\text{al}}}$ ,  $\text{C}_{\text{al-C}_{\text{ar}}}$ ,  $\text{C}_{\text{al-O}}$ ,  $\text{C}_{\text{al-S}}$ , and  $\text{C}_{\text{al-N}}$ , which is not conducive to the decomposition of macromolecules.

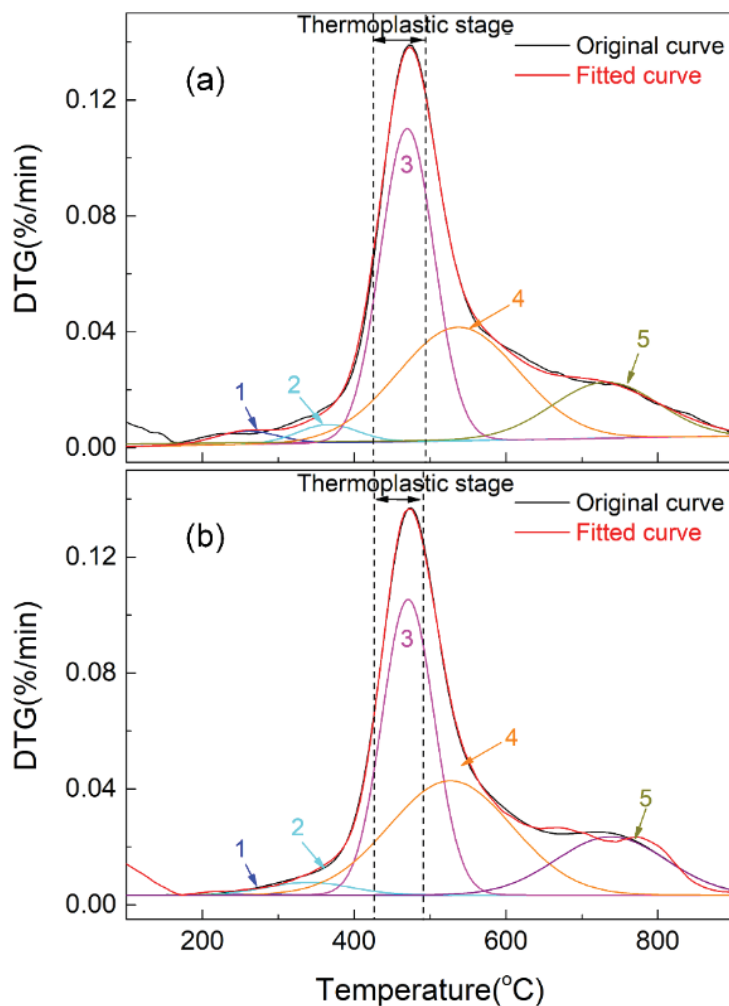


Fig. 3 DTG curves of mixed coal: (a) CM-RAW, (b) CM- $\text{Fe}_2\text{O}_3$ .

**Table 2.** Bond information resulted from the curve-fitting of DTG curves of CM.

Possible origin	temperature range (°C)	CM-RAW			CM-Fe <sub>2</sub> O <sub>3</sub>		
		Peak temperature (°C)	Absolute area	Peak area in thermoplastic stage	Peak temperature (°C)	Absolute area	Peak area in thermoplastic stage
Decomposition of carboxylic acid	<300	258.31	0.48	-	276.23	0.21	-
C <sub>al</sub> -O、C <sub>al</sub> -S、C <sub>al</sub> -N bonds break	300-400	365.22	0.63	0.04	370.49	0.71	0.03
C <sub>al</sub> -C <sub>al</sub> bond break	400-500	469.89	9.56	6.20	468.92	8.62	5.26
C <sub>al</sub> -C <sub>ar</sub> bond break	500-600	536.91	7.81	1.47	526.72	7.21	1.34
C <sub>ar</sub> -H bond break	600-900	750.70	2.48	-	768.32	3.60	-

### 3.3 Changes in the carbon structure of mixed coal during thermoplastic stage after adding Fe<sub>2</sub>O<sub>3</sub>

The XRD spectra of samples is illustrated in Fig. 4. No peaks representing minerals were found in Fig. 4(a), indicating that the removal of minerals by acid treatment achieved as expected. From Fig. 4(b), the diffraction peaks of Fe<sub>2</sub>O<sub>3</sub> and Fe<sub>3</sub>O<sub>4</sub> could be found when CM-Fe<sub>2</sub>O<sub>3</sub> was heated to 400°C and 425°C, further, the diffraction peak of Fe<sub>2</sub>O<sub>3</sub> was disappeared with increasing pyrolysis temperature. It signifies that the added Fe<sub>2</sub>O<sub>3</sub> gradually transforms into Fe<sub>3</sub>O<sub>4</sub> in the thermoplastic stage of coking.

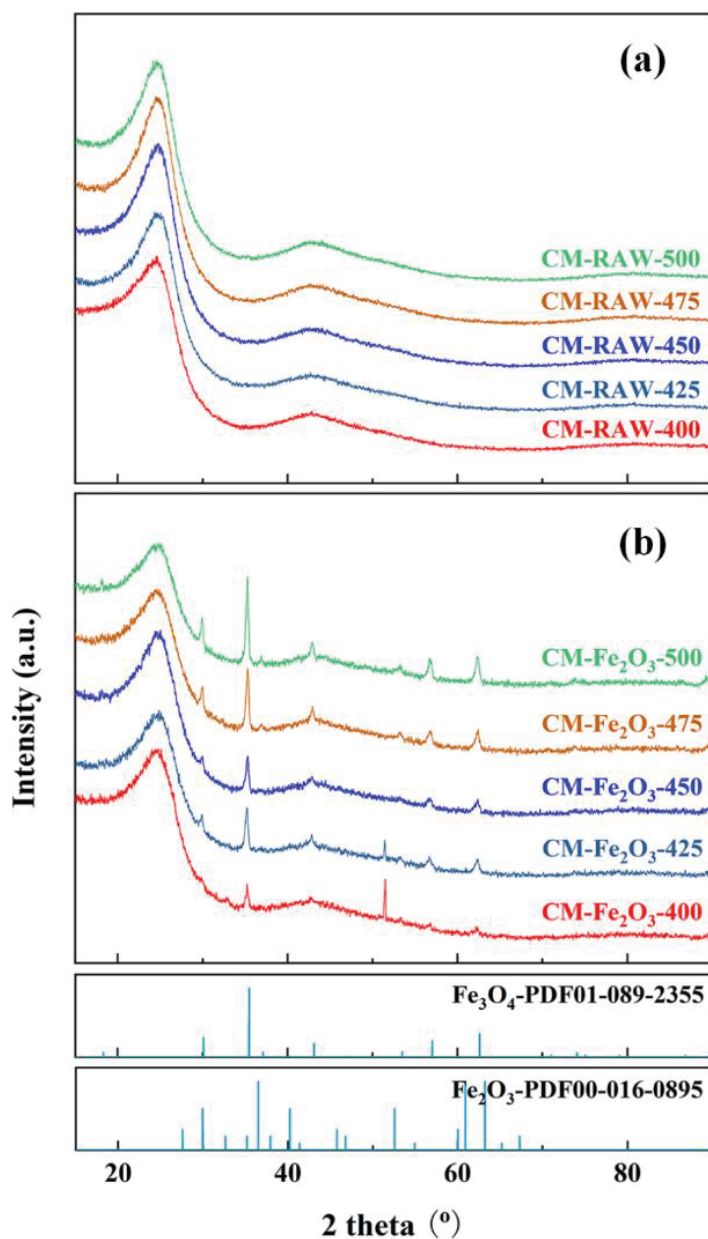


**Fig. 4.** XRD spectra of mixed coal in the thermoplastic stage: (a) CM-RAW, (b) CM-Fe<sub>2</sub>O<sub>3</sub>.

Fig. 5 shows carbon structure of mixed coal after being heated. According to Fig. 5(a), the  $f_a$  values of samples (CM-RAW, CM-Fe<sub>2</sub>O<sub>3</sub>) increased with an increase in temperature, indicating that the aromaticity of mixed coal increases in thermoplastic stage during coking. This may be due to: (a) the alkyl group is decomposed and removed from mixed coal during initial softening stage; (b) some of aliphatic

hydrocarbons undergo a dehydrogenation reaction during the solidification process to form aromatic structures. However, the  $f_a$  value of CM-Fe<sub>2</sub>O<sub>3</sub> decreased compared with the CM-RAW at same temperature, which means the addition of Fe<sub>2</sub>O<sub>3</sub> inhibits the alkyl removal or aromatic dehydrogenation reaction. It can be seen from Fig. 5(b), as pyrolysis temperature increased, the  $d_{002}$  values of samples gradually decreased. The  $d_{002}$  value of CM-Fe<sub>2</sub>O<sub>3</sub> is larger than CM-RAW at same temperature, indicating that the added Fe<sub>2</sub>O<sub>3</sub> inhibits the graphitization of mixed coal in thermoplastic stage. As shown in Fig. 5(c), the values of  $L_c$  increased with an increase in temperature. Furthermore,  $L_c$  value of CM-Fe<sub>2</sub>O<sub>3</sub> is smaller than CM-RAW at same temperature, demonstrating that the added Fe<sub>2</sub>O<sub>3</sub> reduces the average stacking height of mixed coal. Previous study [43] has confirmed that an increase in aromatic clusters helps to accommodate more free radicals. Therefore, the added Fe<sub>2</sub>O<sub>3</sub> could reduce the average stacking height of coal and form less free radicals during coking, which lead to a decrease in the thermoplasticity of mixed coal.



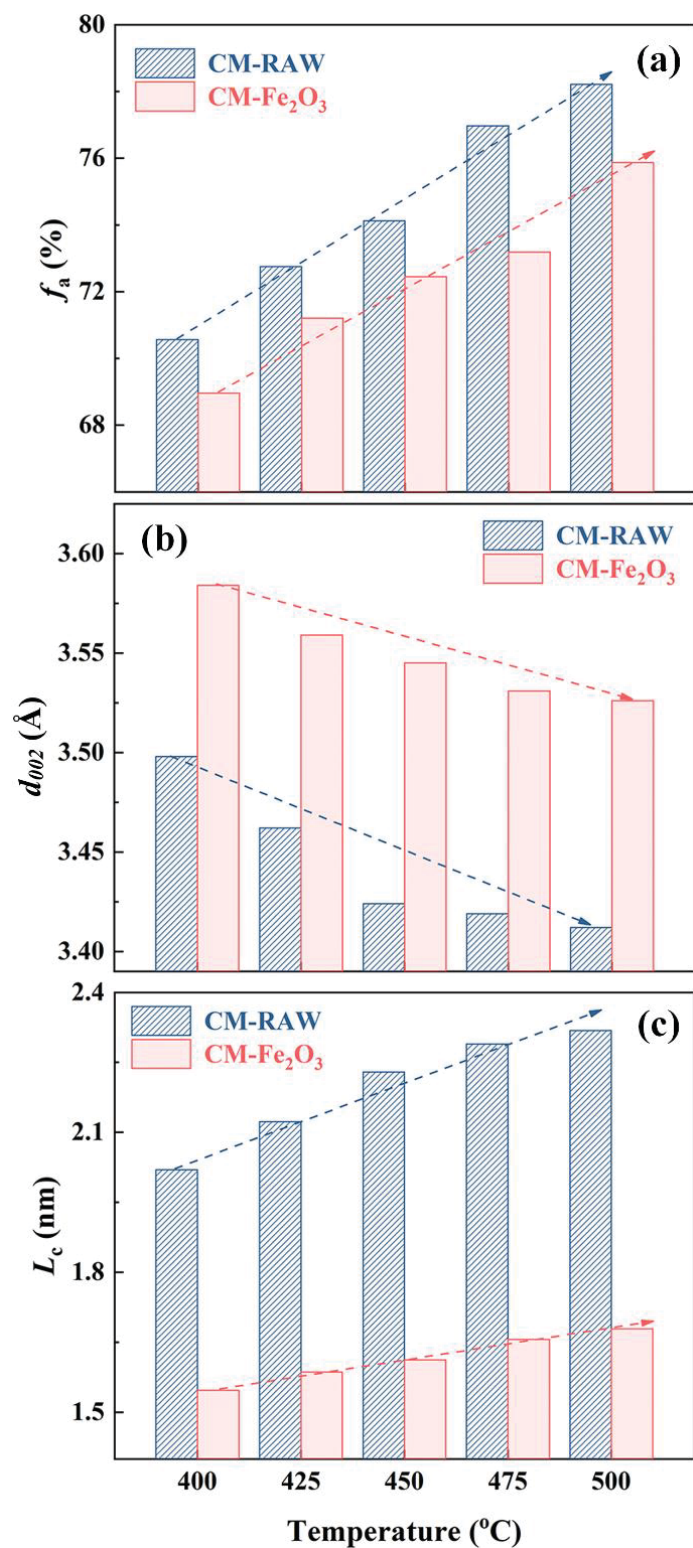


Fig. 5. Structural parameters of mixed coal in thermoplastic stage obtained from XRD spectra: (a) CM- $f_a$ , (b) CM- $d_{002}$ , (c) CM- $L_c$ .



### **3.4. Changes in the structure of functional groups of mixed coal during thermoplastic stage after adding Fe<sub>2</sub>O<sub>3</sub>**

The FT-IR spectra of mixed coal after heating is illustrated in Fig. 6. The spectra show that with an increase in temperature, two vibration peaks representing aliphatic C-H stretching vibrations in the range of 3000-2800 cm<sup>-1</sup> have weakened. It indicates that the large aliphatic compounds of mixed coal are gradually decomposed during pyrolysis process. Moreover, the strength of vibration peak representing C=O and aromatic C=C stretching vibrations in the range of 1700-1500 cm<sup>-1</sup> is also decreased with an increase in temperature. In addition, the vibration peaks of aromatic ether C-O-C and ester O=C-O-C appearing in the range of 1350-1250 cm<sup>-1</sup> are weaker with increasing temperature, indicating that the mixed coal in thermoplastic stage contains a small amount of aromatic ethers and esters. Moreover, many peaks in the range of 950-750 cm<sup>-1</sup> are caused by the out-of-plane deformation of C-H aromatics.

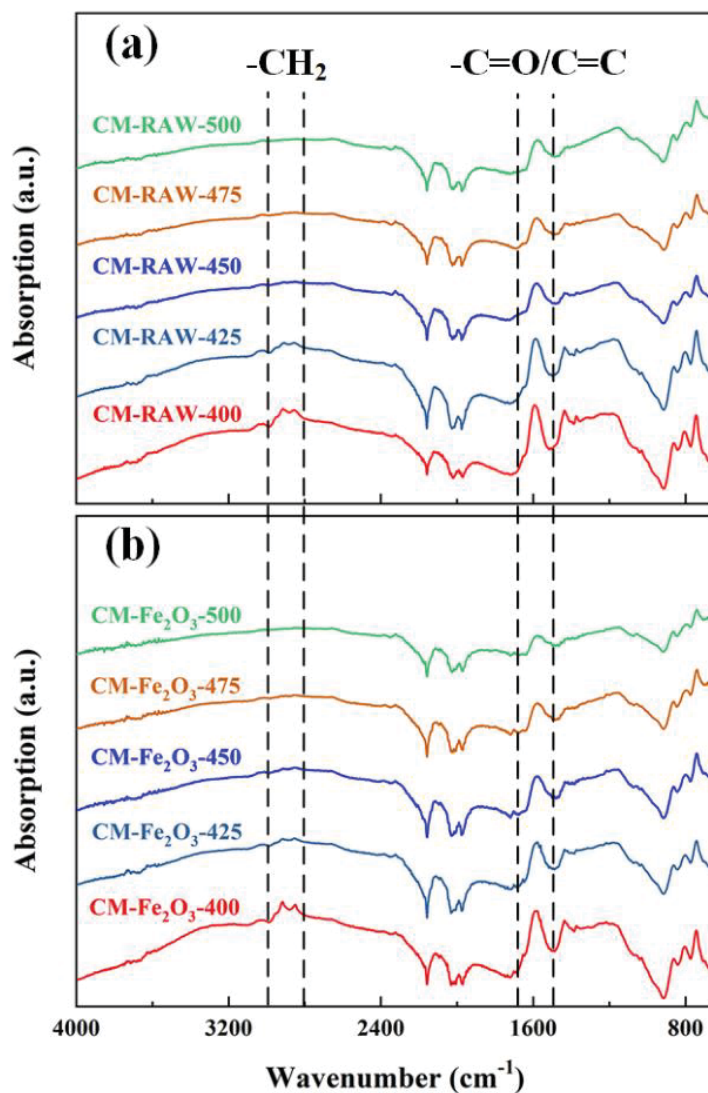


Fig. 6. FT-IR spectra of mixed coal in the thermoplastic stage: (a) CM-RAW, (b) CM-Fe<sub>2</sub>O<sub>3</sub>.

Fig. 7 is obtained by fitting the 3000-2800 cm<sup>-1</sup> and 1700-1500 cm<sup>-1</sup> regions of Fig. 6. In Fig. 7(a), the CH<sub>2</sub>/CH<sub>3</sub> values of samples (CM-RAW, CM-Fe<sub>2</sub>O<sub>3</sub>) decreased first, and then increased with increasing temperatures, indicating that the aliphatic chain length of samples first decreases and then grows during coking. However, the addition of Fe<sub>2</sub>O<sub>3</sub> improved the CH<sub>2</sub>/CH<sub>3</sub> value at the same temperature. This is attributed to Fe<sub>2</sub>O<sub>3</sub> inhibiting the breaking of certain chemical bonds of mixed coal during pyrolysis, such as methylene bridges, chemical bonds connecting aromatic rings to aliphatic side

chain, and chemical bonds connecting small molecules to aliphatic [44]. As shown in Fig. 7(b), the change of *A*-factor value of samples is the reverse of CH<sub>2</sub>/CH<sub>3</sub> value. The *A*-factor value of CM-RAW first raised in the temperature range of 400-450 °C and then decreased, which indicates that hydrocarbon-generating potential of CM-RAW increases, and then decreases during coking. As expected, the *A*-factor value of CM-Fe<sub>2</sub>O<sub>3</sub> is larger than CM-RAW, indicating that the hydrocarbon-generating potential of mixed coal increases with the addition of Fe<sub>2</sub>O<sub>3</sub>. A previous study [45] has confirmed that the aliphatic hydrocarbon linked to the macromolecular structure plays an important role in the thermoplasticity of coal. In this study, the added Fe<sub>2</sub>O<sub>3</sub> inhibited the decomposition of C<sub>al</sub>-C<sub>al</sub>, C<sub>al</sub>-C<sub>ar</sub>, C<sub>al</sub>-O, C<sub>al</sub>-S, and C<sub>al</sub>-N during coking, resulting in the increase of CH<sub>2</sub>/CH<sub>3</sub> and *A*-factor of mixed coal, which ultimately decreases the thermoplasticity of mixed coal.

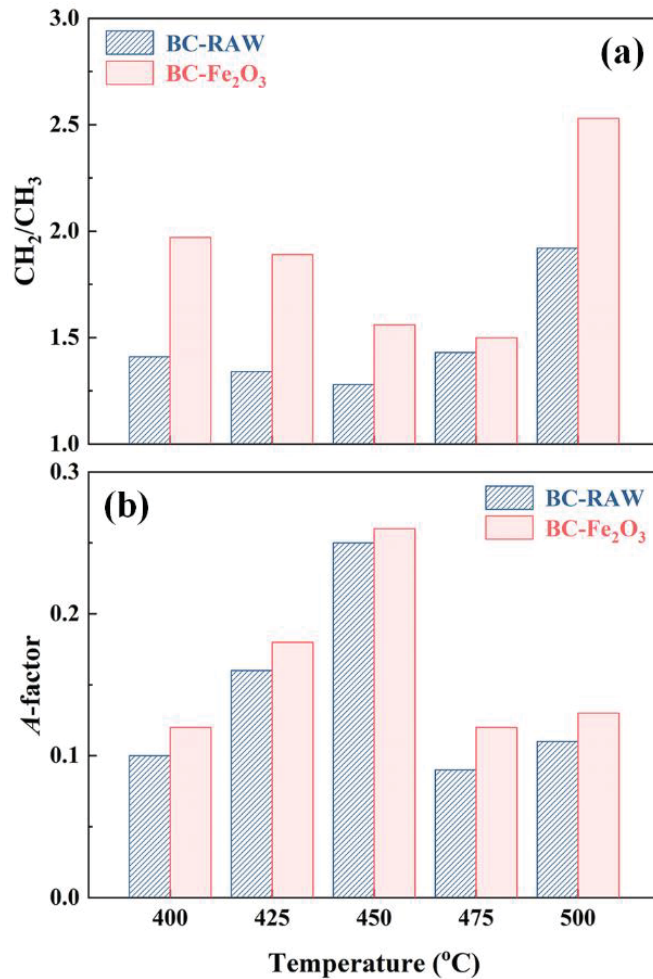


Fig. 7. Structure parameters of mixed coal in the thermoplastic stage: (a) CM- $CH_2/CH_3$ , (b) CM-A-factor.

### 3.5. Changes in the fluid phase transformation of mixed coal during thermoplastic stage after adding Fe<sub>2</sub>O<sub>3</sub>

It can be seen from Fig. 8 that the contents of light and heavy extract of samples (CM-RAW, CM-Fe<sub>2</sub>O<sub>3</sub>) both increased first and then decreased, and finally reached to the maximum at 450 °C. But the heavy extract content of samples is much higher than light extract. After adding Fe<sub>2</sub>O<sub>3</sub>, the maximum contents of light and heavy extract of mixed coal is 1.90% and 8.27%, respectively, which is 1.4% and 1.0% lower than CM-RAW respectively.

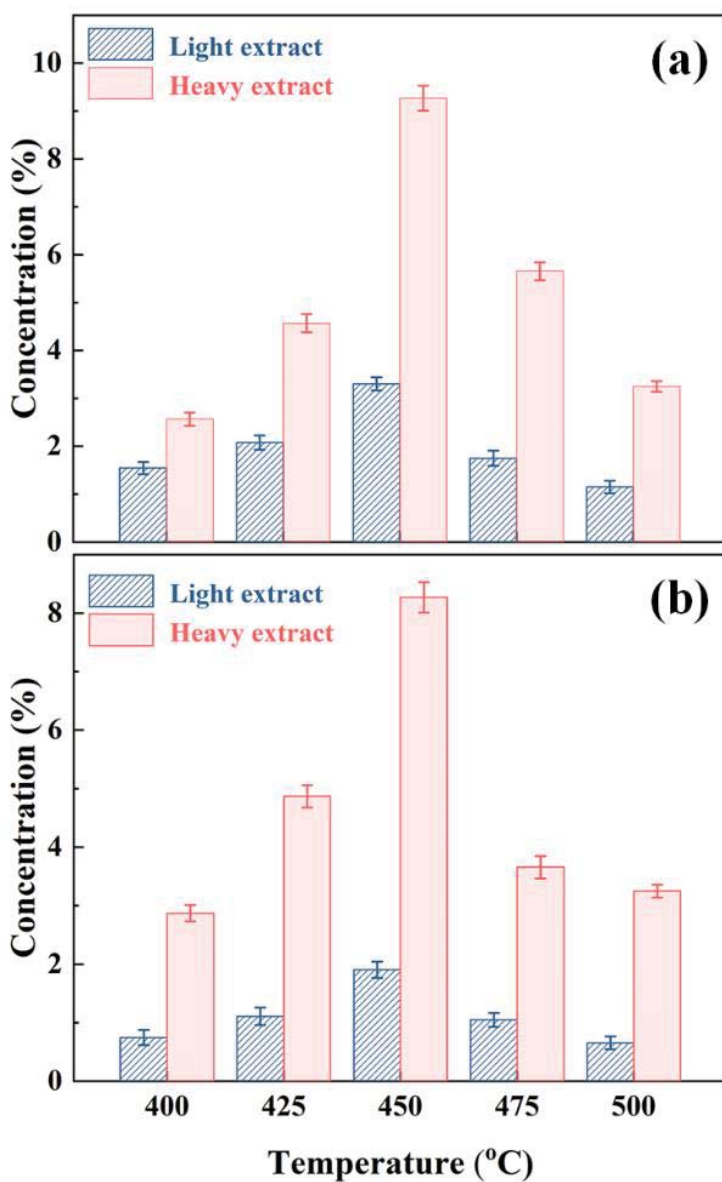
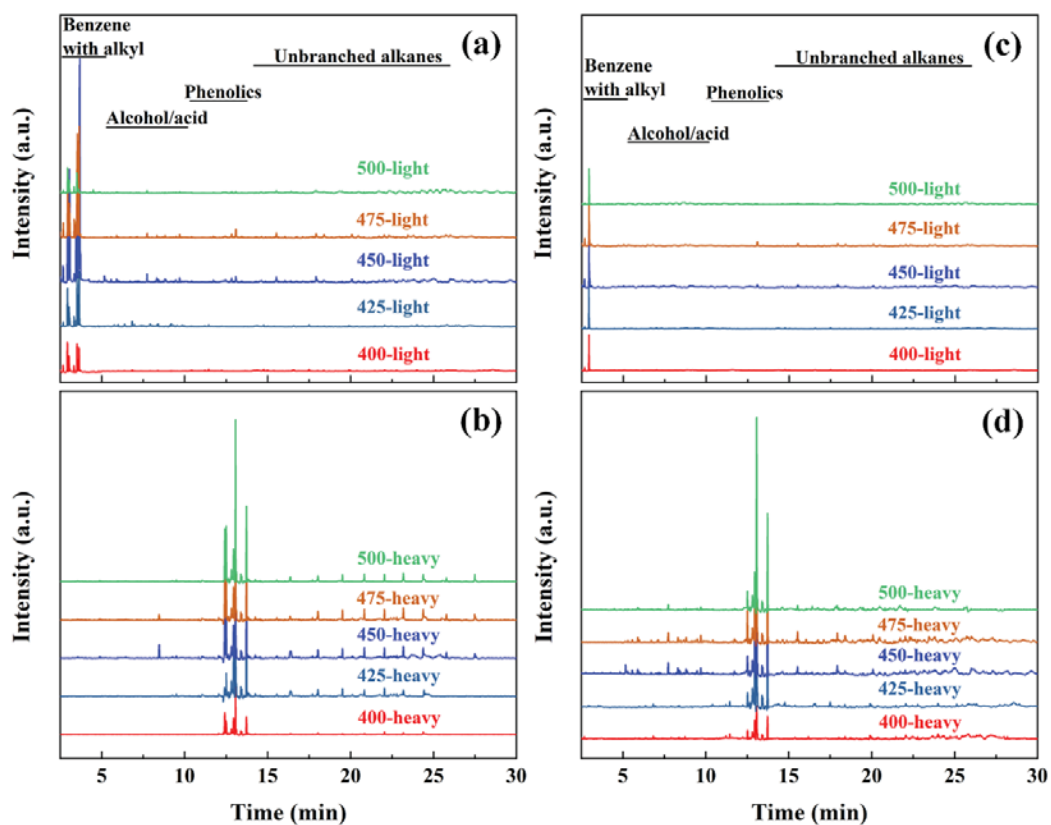


Fig. 8. Concentrations of light and heavy extract in the thermoplastic stage: (a) CM-RAW, (b) CM-Fe<sub>2</sub>O<sub>3</sub>.

Fig. 9 shows GC-MS chromatograms of samples extracts (CM-RAW, CM-Fe<sub>2</sub>O<sub>3</sub>). The detailed compounds information is shown in Table 3, Table 4, Table 5 and Table 6. According to the previous study [26], it can be seen from Fig. 9(a) and Table 3 that the components of the light extract of heated mixed coal in the thermoplastic stage are mainly included methylbenzene, ethylbenzene, o-xylene, 4-hydroxybutyric acid and

Pantolactone, and light fluid phase is mainly composed of methylbenzene, ethylbenzene and o-xylene. It can be observed from Fig. 9(c) and Table 4 that after adding Fe<sub>2</sub>O<sub>3</sub>, the main substances of light extract are 2-pentanone and methylbenzene during thermoplastic stage, and the light fluid phase of mixed coal containing Fe<sub>2</sub>O<sub>3</sub> is mainly consist of methylbenzene. As shown in Fig. 9(b) and Table 5, the heavy extract are mainly phenolic compounds and unbranched alkanes, such as 3-(1,1-dimethylethyl)-4-methyl-phenol, 4-methyl-2-phenol, 2,6-bis(1,1-dimethylethyl)-p-cresol and carbon number are 19-26 unbranched alkanes. Furthermore, the heavy fluid phase is unbranched alkanes with 19-26 carbon atoms. It can be seen from Fig. 9(d) and Table 6, the heavy extract of mixed coal containing Fe<sub>2</sub>O<sub>3</sub> mainly consists of phenolic compounds, alkyd compounds and unbranched alkanes, which are mainly nonadecane, docosane, and tricosane, however, the heavy fluid phase mainly consists of nonadecane, docosane, tricosane and alkyd compounds.



**Fig. 9.** GC-MS chromatograms of the extract obtained from CM in the thermoplastic stage; (a) CM-RAW light extract, (b) CM-RAW heavy extract, (c) CM-Fe<sub>2</sub>O<sub>3</sub> light extract, and (d) CM-Fe<sub>2</sub>O<sub>3</sub> heavy extract.

**Table 3.** Chemical compounds in light extract obtained from CM-RAW.

Time(min)	Compounds	Light extract of CM-RAW (%)				
		400	425	450	475	500
2.66	2-Pentanone	8.12	5.18	6.62	5.81	2.13
2.97	Methylbenzene*	16.12	19.82	21.15	18.64	15.98
3.04	Ethylbenzene *	12.15	20.22	25.33	21.15	19.67
3.33	O-xylene*	18.47	21.05	22.34	21.41	19.13
3.50	4-Hydroxybutanoic acid	29.21	21.41	11.08	13.45	15.34
3.60	Pantolactone	15.93	12.32	6.25	12.16	15.39
7.49	Pyridine	-	-	1.88	1.52	3.15
9.68	2,3-dimethyl-Dodecane	-	-	1.21	1.07	3.26
13.09	2,6-bis (1,1-dimethylethyl) -p-Cresol	-	-	2.02	2.81	3.61
15.50	Eicosane			2.12	1.98	2.34

\*: light fluid phase, 400: the light extract obtained from mixed coal at the pyrolysis temperature of 400°C.

**Table 4.** Chemical compounds in light extract obtained from CM-Fe<sub>2</sub>O<sub>3</sub>.

Time(min)	Compounds	Light extract of CM-Fe <sub>2</sub> O <sub>3</sub> (%)				
		400	425	450	475	500
2.66	2-Pentanone	10.23	8.46	11.52	13.34	8.21
2.97	Methylbenzene*	89.77	92.54	88.48	86.66	91.79

\*: light fluid phase, 400: the light extract obtained from mixed coal at a temperature of 400 °C.

**Table 5.** Chemical compounds in heavy extract obtained from CM-RAW.

Time(min)	Compounds	Heavy extract of CM-RAW (%)				
		400	425	450	475	500
8.56	4-hydroxy- Butanoic acid <sup>#</sup>	-	-	6.13	3.56	-
12.09	2,6-bis(1,1-dimethylethyl)-p-Benzoquinone	-	3.36	-	-	1.99
12.44	3-(1,1-dimethylethyl)-4-methyl-Phenol	16.14	9.14	14.25	15.38	17.18
12.64	4-methyl-2-Phenol	9.09	6.86	3.31	2.69	2.34
13.09	2,6-bis(1,1-dimethylethyl)-p-Cresol	56.54	33.65	17.29	17.59	29.47
13.70	2-methyl-2-(3-methyl-2-butoxyl) - Cyclohexanone	12.23	8.52	17.12	18.14	19.07
14.37	Nonadecane <sup>#</sup>	1.14	-	2.19	1.95	1.97
16.10	Docosane <sup>#</sup>	-	5.13	5.54	4.98	2.49
16.67	Tricosane <sup>#</sup>	-	3.24	3.36	2.09	1.67
18.08	Tetracosane <sup>#</sup>	-	5.34	5.61	5.12	2.57
19.51	6-methyl-Tetracosane <sup>#</sup>	-	4.28	4.01	4.68	3.29
20.79	Pentacosane <sup>#</sup>	-	4.56	4.51	4.72	2.53
22.04	3-methyl-Pentacosane <sup>#</sup>	2.53	5.88	4.95	4.19	3.27
23.18	5-ethyl-Pentacosane <sup>#</sup>	2.33	6.03	4.38	5.14	2.96
24.24	Hexacosane <sup>#</sup>	-	4.01	3.12	3.21	3.15
25.81	6-methyl-Hexacosane <sup>#</sup>	-	-	2.16	3.35	2.91
26.85	Perylene	-	-	2.07	3.21	3.14

<sup>#</sup>: heavy fluid phase compounds, 400: the heavy extract obtained from mixed coal at a temperature of 400 °C.

**Table 6.** Chemical compounds in heavy extract obtained from CM-Fe<sub>2</sub>O<sub>3</sub>.

Time(min)	Compounds	Heavy extract of CM-Fe <sub>2</sub> O <sub>3</sub> (%)				
		400	425	450	475	500
8.56	4-hydroxy- Butanoic acid <sup>#</sup>	-	-	1.98	1.26	0.98
9.44	5-Hexene- Acetic acid <sup>#</sup>	-	-	2.02	1.62	-
11.96	2,6-bis(3,5-di-tert-butyl-4-hydroxybenzyl)-Phenol	3.24	-	3.86	3.98	2.52
12.09	2,6-bis(1,1-dimethylethyl)-p	11.01	12.98	13.01	19.34	10.59



Time(min)	Compounds	Heavy extract of CM-Fe <sub>2</sub> O <sub>3</sub> (%)				
		400	425	450	475	500
	-Benzoquinone					
12.44	3-(1,1-dimethylethyl)-4-methyl-Phenol	20.15	21.58	18.24	17.92	10.52
12.64	4-methyl-2-Phenol	9.16	10.25	7.35	6.57	8.34
13.09	2,6-bis(1,1-dimethylethyl)-p-Cresol	25.97	27.85	26.59	23.49	41.86
13.70	2-methyl-2-(3-methyl-2-butoxyl) -Cyclohexanone	20.65	18.21	17.24	16.58	20.18
14.37	Nonadecane <sup>#</sup>	3.45	3.14	2.25	4.87	2.56
16.10	Docosane <sup>#</sup>	4.21	3.19	4.27	2.19	1.38
16.67	Tricosane <sup>#</sup>	2.16	2.8	3.19	2.47	1.07

<sup>#</sup>: heavy fluid phase compounds, 400: the heavy extract obtained from mixed coal at temperature of 400°C.

Therefore, from the changes in fluid phase composition of mixed coal after adding Fe<sub>2</sub>O<sub>3</sub>, the main effect of Fe<sub>2</sub>O<sub>3</sub> on the specific compounds during thermoplastic stage was obtained [46, 47]. Monocyclic benzene compounds (methylbenzene) are mainly generated by the reaction of decomposed complex polycyclic benzene compounds with small molecular gases. Previous work confirmed that during the pyrolysis of coal, C-C bond between benzene rings decomposed first, generating highly reactive aromatic free radicals and some small molecular gases (CH<sub>4</sub>, H<sub>2</sub>, and C<sub>2</sub>H<sub>2</sub>) [48, 49]. However, the added Fe<sub>2</sub>O<sub>3</sub> inhibited these processes, as evidenced by decline of C<sub>al</sub>-C<sub>ar</sub> in the DTG analysis. Only methylbenzene was detected in the light extract of mixed coal after adding Fe<sub>2</sub>O<sub>3</sub>, while ethylbenzene and o-xylene disappeared. Therefore, it is considered that the added Fe<sub>2</sub>O<sub>3</sub> inhibits the formation of ethylbenzene and o-xylene in the light fluid phase during coking. At the same time, the aliphatic side chains connected to the coal matrix are broken to generate aliphatic free radicals when mixed coal is heated. But the cleavage of C<sub>al</sub>-C<sub>al</sub> is inhibited by the addition of Fe<sub>2</sub>O<sub>3</sub>, which reduces the formation of aliphatic free radicals, thereby reducing the formation of unbranched

alkanes with 24-26 carbon atoms in the heavy fluid phase.

Fig. 10 shows changes in the fluid phase content based on the weight of mixed coal in the thermoplastic stage after adding  $\text{Fe}_2\text{O}_3$ . The relative content of light and heavy fluid phases of samples (CM-RAW, CM- $\text{Fe}_2\text{O}_3$ ) increased with an increase of temperature in the range of 400-450°C, and then decreased. Moreover, the change of heavy fluid phase is larger than that of the light fluid phase. However, the addition of  $\text{Fe}_2\text{O}_3$  greatly reduced the content of fluid phase of mixed coal (at 450°C, the light and heavy fluid phases were reduced by 0.59% and 3.09%, respectively), resulting in the fluidity of mixed coal decreases in thermoplastic stage.

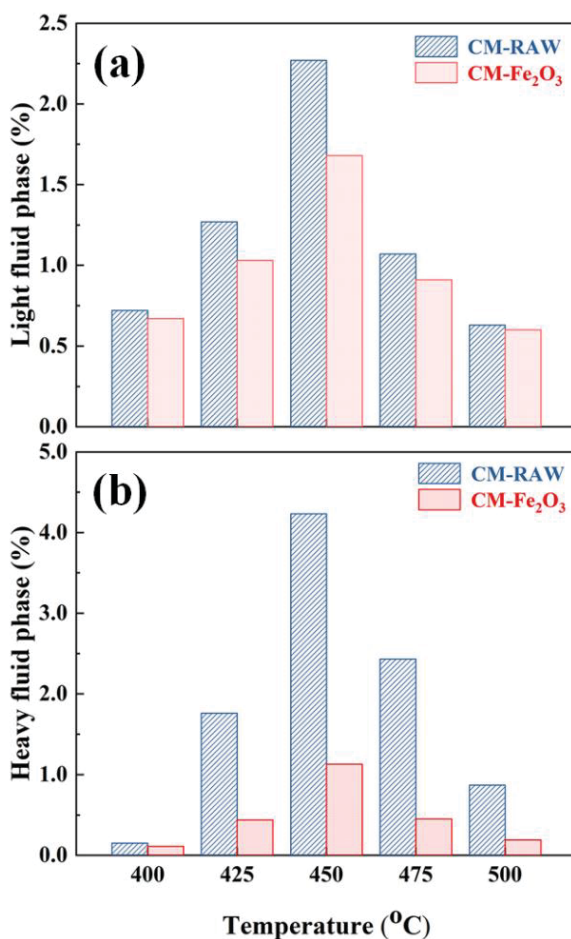


**Fig. 10.** The concentration of fluid phase of mixed coal in the thermoplastic stage based on the weight of mixed coal: (a) light fluid phase, and (b) heavy fluid phase.

### 3.6. Strength degradation mechanism of iron coke prepared by mixed coal and $\text{Fe}_2\text{O}_3$

As a macromolecular unit, the chemical structure of coal matrix has many chemical bonds, such as -C-C-, -CH<sub>2</sub>-, -CH-, -O-, and -S-. which are intertwined and connected. In addition, these macromolecular units are also connected to low molecular weight substances through bond bridges. In the coking process, the depolymerization of coal mainly occurs on the side chains or bridge between the basic structural unit of coal and low molecular weight compounds, thereby generating fluid phase and a small amount of coal tar [47]. Based on our previous work [26], the components of fluid phase are mainly monocyclic benzene and long chain unbranched alkanes, and the following structural changes occur in the thermoplastic stage: (a) the formation and stabilization of fluid phase, (b) cross-linking and re-attaching of the fluid phase to coal char.

Fig. 11 shows the strength degradation mechanism of iron coke [45-50]. When the mixed coal is within the thermoplastic temperature range, the bonds of C<sub>al</sub>-O, C<sub>al</sub>-S, C<sub>al</sub>-N, C<sub>al</sub>-C<sub>ar</sub>, and C<sub>al</sub>-C<sub>al</sub> in macromolecular units or between macromolecular units and low molecules will be broken, producing low molecular weight aromatic and aliphatic free radicals. However, when  $\text{Fe}_2\text{O}_3$  was added, the cleavage of C<sub>al</sub>-O, C<sub>al</sub>-S, C<sub>al</sub>-N, C<sub>al</sub>-C<sub>ar</sub>, and C<sub>al</sub>-C<sub>al</sub> was inhibited, leading to the reduction of aromatic and aliphatic free radicals. This hinders the formation of monocyclic benzene compounds (ethylbenzene and o-xylene) and linear alkanes (24-26 carbon atoms) at stage (a), leading to a decrease in the content of fluid phase, which in turn reduces the aromaticity and average stacking height, and increases the interlayer spacing, aliphatic chain length, and hydrocarbon generation potential of mixed coal. At stage (b), due to the decrease in the content of

fluid phase, hydrogen migration-acetylene addition reaction and crosslinking reaction of monocyclic benzene compounds in the fluid phase are weakened, and the formation of complex compounds is reduced. However, as the macromolecular substances of mixed coal did not decompose in the thermoplastic stage, the side group still existed in large quantities, leading to an increase in the hydrocarbon generation ability and aliphatic chain length, a decrease in the maximum fluidity and the thermoplastic stage of coal, and ultimately a reduction in coke strength.

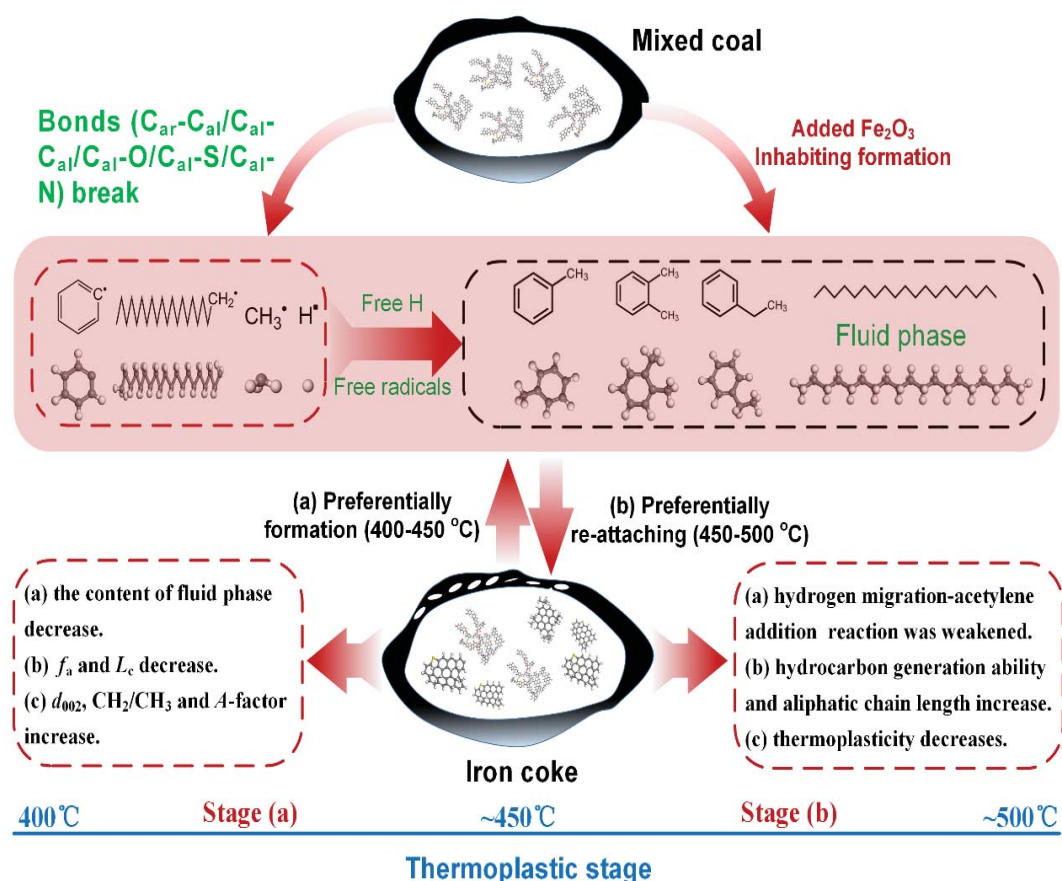


Fig. 11. Strength degradation mechanism of iron coke prepared by mixed coal and  $Fe_2O_3$  [45-50].

## 4. Conclusions

This study shed light on the strength degradation mechanism of iron coke through Gieseler plastometer, TGA, XRD, FT-IR and GC-MS analysis. It was found that the addition of  $\text{Fe}_2\text{O}_3$  hinders the cleavage of  $\text{C}_{\text{al-O}}$ ,  $\text{C}_{\text{al-S}}$ ,  $\text{C}_{\text{al-N}}$ ,  $\text{C}_{\text{al-Car}}$  and  $\text{C}_{\text{al-Cal}}$ , thereby inhibiting the formation of ethylbenzene, o-xylene and unbranched alkanes with carbon atoms in 24-26, and ultimately reduces the amount of fluid phase during coking. At the same time, the inhibition of  $\text{Fe}_2\text{O}_3$  decreases the aromaticity and average stacking height increases the interlayer spacing of the crystallite, aliphatic chain length and hydrocarbon-generating potential of mixed coal. Finally, the above changes combined to reduce the fluidity and thermoplastic range of the mixed coal after adding  $\text{Fe}_2\text{O}_3$ , resulting in the strength degradation of iron coke.

## Acknowledgements

The authors thank the National Natural Science Foundation of China (Grant Nos. 51474042 & 51774061) and the Fundamental Research Funds for Central Universities (Grant No. 106112017CDJQJ138801) for financial support.

## References

- [1] D.M. Kundrat, T. Miwa, A. Rist, Injections in the iron blast furnace: a graphics study by means of the rist operating diagram, *Metallurgical Transactions B-Process Metallurgy*, 22 (1991) 363-383. <https://doi.org/10.1007/bf02651235>.
- [2] T. Ariyama, R. Murai, J. Ishii, M. Sato, Reduction of CO<sub>2</sub> emissions from integrated steel works and its subjects for a future study, *Isij International*, 45 (2005) 1371-1378. <https://doi.org/10.2355/isijinternational.45.1371>.
- [3] K.C. Xie, *Structure and reactivity of coal*, Springer, Berlin, Heidelberg, 2015. <https://doi.org/10.1007/978-3-662-47337-5>.
- [4] Y. Ohtsuka, Y. Kuroda, Y. Tamai, A. Tomita, Chemical form of iron catalysts during the CO<sub>2</sub>-gasification of carbon, *Fuel*, 65 (1986) 1476-1478. [https://doi.org/10.1016/0016-2361\(86\)90128-6](https://doi.org/10.1016/0016-2361(86)90128-6).
- [5] K. Miura, K. Hashimoto, P.L. Silveston, Factors affecting the reactivity of coal chars during gasification, and indexes representing reactivity, *Fuel*, 68 (1989) 1461-1475. [https://doi.org/10.1016/0016-2361\(89\)90046-x](https://doi.org/10.1016/0016-2361(89)90046-x).
- [6] D. Cazorlaamoros, A. Linaressolano, C.S. Delecea, Carbon gasification catalyzed by calcium - a high-vacuum temperature programmed desorption study, *Carbon*, 30 (1992) 995-1000. [https://doi.org/10.1016/0008-6223\(92\)90127-i](https://doi.org/10.1016/0008-6223(92)90127-i).
- [7] L. Lahaye, P. Ehrburger, *Fundamental issues in control of carbon gasification reactivity*, Berlin: Springer Science & Business Media, 2012.
- [8] S. Nomura, H. Ayukawa, H. Kitaguchi, T. Tahara, S. Matsuzaki, M. Naito, S. Koizumi, Y. Ogata, T. Nakayama, T. Abe, Improvement in blast furnace reaction efficiency through the use of highly reactive calcium rich coke, *Isij International*, 45 (2005) 316-324.

<https://doi.org/10.2355/isijinternational.45.316>.

[9] S. Nomura, M. Naito, K. Yamaguchi, Post-reaction strength of catalyst-added highly reactive coke, *Isij International*, 47 (2007) 831-839. <https://doi.org/10.2355/isijinternational.47.831>.

[10] K. Higuchi, S. Nomura, K. Kunitomo, H. Yokoyama, M. Naito, Enhancement of Low-temperature Gasification and Reduction by Using Iron-coke in Laboratory Scale Tests, *Isij International*, 51 (2011) 1308-1315. <https://doi.org/10.2355/isijinternational.51.1308>.

[11] H. Wang, M. Chu, Z. Wang, W. Zhao, Z. Liu, J. Tang, Z. Ying, Research on the post-reaction strength of iron coke hot briquette under different conditions, *Jom*, 70 (2018) 1929-1936. <https://doi.org/10.1007/s11837-018-3036-4>.

[12] H. Wang, W. Zhao, M. Chu, Z. Liu, J. Tang, Z. Ying, Effects of coal and iron ore blending on metallurgical properties of iron coke hot briquette, *Powder Technology*, 328 (2018) 318-328. <https://doi.org/10.1016/j.powtec.2018.01.027>.

[13] R. Xu, B. Dai, W. Wang, J. Schenk, Z. Xue, Effect of iron ore type on the thermal behaviour and kinetics of coal-iron ore briquettes during coking, *Fuel Processing Technology*, 173 (2018) 11-20. <https://doi.org/10.1016/j.fuproc.2018.01.006>.

[14] R. Xu, H. Zheng, W. Wang, J. Schenk, Z. Xue, Influence of iron minerals on the volume, strength, and CO<sub>2</sub> gasification of ferro-coke, *Energy & Fuels*, 32 (2018) 12118-12127. <https://doi.org/10.1021/acs.energyfuels.8b02644>.

[15] H. Zheng, W. Wang, R. Xu, R. Zan, J. Schenk, Z. Xue, Effect of the Particle Size of Iron Ore on the Pyrolysis Kinetic Behaviour of Coal-Iron Ore Briquettes, *Energies*, 11 (2018). <https://doi.org/10.3390/en11102595>.

[16] H. Wang, M. Chu, B. Guo, J. Bao, W. Zhao, Z. Liu, J. Tang, Investigation on Gasification Reaction Behavior and Kinetic Analysis of Iron Coke Hot Briquette under Isothermal Conditions,

- Steel Research International, 90 (2019). <https://doi.org/10.1002/srin.201800354>.
- [17] H. Wang, M. Chu, W. Zhao, Z. Liu, J. Tang, Influence of Iron Ore Addition on Metallurgical Reaction Behavior of Iron Coke Hot Briquette, Metallurgical and Materials Transactions B-Process Metallurgy and Materials Processing Science, 50 (2019) 324-336. <https://doi.org/10.1007/s11663-018-1481-7>.
- [18] M.A. Diez, R. Alvarez, C. Barriocanal, Coal for metallurgical coke production: predictions of coke quality and future requirements for cokemaking, International Journal of Coal Geology, 50 (2002) 389-412. [https://doi.org/10.1016/s0166-5162\(02\)00123-4](https://doi.org/10.1016/s0166-5162(02)00123-4).
- [19] Q. Zhang, X.C. Wu, A.Z. Feng, M.R. Shi, Prediction of coke quality at Baosteel, Fuel Processing Technology, 86 (2004) 1-11. [https://doi.org/10.1016/s0378-3820\(03\)00058-4](https://doi.org/10.1016/s0378-3820(03)00058-4).
- [20] L. North, K. Blackmoreb, K. Nesbitt, M.R. Mahoney, Models of coke quality prediction and the relationships to input variables: A review, Fuel, 219 (2018) 446-466. <https://doi.org/10.1016/j.fuel.2018.01.062>.
- [21] M.R. Khan, P.L. Walker, R.G. Jenkins, Swelling and plastic properties of coal devolatilized at elevated pressures of H<sub>2</sub> and He: influences of added iron-oxides, Fuel, 67 (1988) 693-699. [https://doi.org/10.1016/0016-2361\(88\)90301-8](https://doi.org/10.1016/0016-2361(88)90301-8).
- [22] A. Uchida, Y. Yamazaki, K. Hiraki, T. Kanai, Y. Saito, H. Aoki, T. Inoue, N. Kikuchi, N. Okuyama, M. Hamaguchi, Evaluation of Properties of Hyper-coal with Iron Oxide Addition in Thermoplastic Range, Isij International, 53 (2013) 1165-1171. <https://doi.org/10.2355/isijinternational.53.1165>.
- [23] R. Stanger, J. Borrowdale, N. Smith, W. Xei, T. Quang Anh, J. Lucas, T. Wall, Changes in Solvent-Extracted Matter for Heated Coal during Metaplast Formation Using High-Range Mass Spectrometry, Energy & Fuels, 29 (2015) 7101-7113. <https://doi.org/10.1021/acs.energyfuels.5b01850>.
- [24] R. Stanger, T. Quang Anh, T. Attalla, N. Smith, J. Lucas, T. Wall, The pyrolysis behaviour of solvent extracted metaplast material from heated coal using LDI-TOF mass spectroscopy



- measurements, *Journal of Analytical and Applied Pyrolysis*, 120 (2016) 258-268.  
<https://doi.org/10.1016/j.jaap.2016.05.014>.
- [25] R. Stanger, T. Quang Anh, W. Xie, N. Smith, J. Lucas, J. Yu, E. Kennedy, M. Stockenhuber, T. Wall, The use of LDI-TOF imaging mass spectroscopy to study heated coal with a temperature gradient incorporating the plastic layer and semi-coke, *Fuel*, 165 (2016) 33-40.  
<https://doi.org/10.1016/j.fuel.2015.10.028>.
- [26] S.X. Qiu, S.F. Zhang, Y. Wu, G.B. Qiu, C.G. Sun, Q.Y. Zhang, J. Dang, L.Y. Wen, M.L. Hu, J. Xu, R.J. Zhu, C.G. Bai, Structural transformation of fluid phase extracted from coal matrix during thermoplastic stage of coal pyrolysis, *Fuel*, 232 (2018) 374-383.  
<https://doi.org/10.1016/j.fuel.2018.05.136>.
- [27] S.X. Qiu, S.F. Zhang, Q.Y. Zhang, G.B. Qiu, L.Y. Wen, Effects of iron compounds on pyrolysis behavior of coals and metallurgical properties of resultant cokes, *Journal of Iron and Steel Research International*, 24 (2017) 1169-1176. [https://doi.org/10.1016/S1006-706X\(18\)30014-1](https://doi.org/10.1016/S1006-706X(18)30014-1).
- [28] S.X. Qiu, S.F. Zhang, R.J. Zhu, Yue Wu, G.B. Qiu, J. Dang, L.Y. Wen, M.L. Hu, C.G. Bai, Influence of TiO<sub>2</sub> addition on the structure and metallurgical properties of coke, *International Journal of Coal Preparation and Utilization*, (2018).  
<https://doi.org/10.1080/19392699.2018.1496913>.
- [29] S. Gupta, V. Sahajwalla, J. Burgo, P. Chaubal, T. Youmans, Carbon structure of coke at high temperatures and its influence on coke fines in blast furnace dust, *Metallurgical and Materials Transactions B-Process Metallurgy and Materials Processing Science*, 36 (2005) 385-394.  
<https://doi.org/10.1007/s11663-005-0067-3>.
- [30] S. Gupta, D. French, R. Sakurovs, M. Grigore, H. Sun, T. Cham, T. Hilding, M. Hallin, B. Lindblom, V. Sahajwalla, Minerals and iron-making reactions in blast furnaces, *Progress in Energy and Combustion Science*, 34 (2008) 155-197. <https://doi.org/10.1016/j.pecs.2007.04.001>.

- [31] S.X. Qiu, S.F. Zhang, Y.P. Fang, G.B. Qiu, C. Yin, R.G. Reddy, Q. Zhang, L.Y. Wen, Effects of poplar addition on tar formation during the co-pyrolysis of fat coal and poplar at high temperature, *RSC Advances*, 9 (2019) 28053-28060. <https://doi.org/10.1039/c9ra03938d>.
- [32] F. Gayo, R. Garcia, M.A. Diez, Modelling the Gieseler fluidity of coking coals modified by multicomponent plastic wastes, *Fuel*, 165 (2016) 134-144. <https://doi.org/10.1016/j.fuel.2015.10.053>.
- [33] T.P. Eskay, P.F. Britt, A.C. Buchanan, Pyrolysis of aromatic carboxylic acids: Potential involvement of anhydrides in retrograde reactions in low-rank coal, *Energy & Fuels*, 11 (1997) 1278-1287. <https://doi.org/10.1021/ef9700745>.
- [34] F. Meng, S. Gupta, J. Yu, Y. Jiang, P. Koshy, C. Sorrell, Y. Shen, Effects of kaolinite addition on the thermoplastic behaviour of coking coal during low temperature pyrolysis, *Fuel Process. Technol.*, 167 (2017) 502-510. <https://doi.org/10.1016/j.fuproc.2017.08.005>.
- [35] K. Miura, K. Mae, W. Li, T. Kusakawa, F. Morozumi, A. Kumano, Estimation of hydrogen bond distribution in coal through the analysis of OH stretching bands in diffuse reflectance infrared spectrum-measured by in-situ technique, *Energy & Fuels*, 15 (2001) 599-610. <https://doi.org/10.1021/ef0001787>.
- [36] K. Miura, K. Mae, M. Shimada, H. Minami, Analysis of formation rates of sulfur-containing gases during the pyrolysis of various coals, *Energy & Fuels*, 15 (2001) 629-636. <https://doi.org/10.1021/ef000185v>.
- [37] L. Shi, Q. Liu, X. Guo, W. Wu, Z. Liu, Pyrolysis behavior and bonding information of coal - A TGA study, *Fuel Process. Technol.*, 108 (2013) 125-132. <https://doi.org/10.1016/j.fuproc.2012.06.023>.
- [38] B. Tian, Y. Qiao, X. Lin, Y. Jiang, L. Xu, X. Ma, Y. Tian, Correlation between bond structures

and volatile composition of Jining bituminous coal during fast pyrolysis, *Fuel Process. Technol.*, 179 (2018) 99-107. <https://doi.org/10.1016/j.fuproc.2018.06.019>.

[39] B. Tian, Y.-y. Qiao, Y.-y. Tian, Q. Liu, Investigation on the effect of particle size and heating rate on pyrolysis characteristics of a bituminous coal by TG-FTIR, *Journal of Analytical and Applied Pyrolysis*, 121 (2016) 376-386. <https://doi.org/10.1016/j.jaap.2016.08.020>.

[40] A. Arenillas, C. Pevida, F. Rubiera, R. Garcia, J.J. Pis, Characterisation of model compounds and a synthetic coal by TG/MS/FTIR to represent the pyrolysis behaviour of coal, *Journal of Analytical and Applied Pyrolysis*, 71 (2004) 747-763. <https://doi.org/10.1016/j.jaap.2003.10.005>.

[41] Q. Liu, S. Wang, Y. Zheng, Z. Luo, K. Cen, Mechanism study of wood lignin pyrolysis by using TG-FTIR analysis, *Journal of Analytical and Applied Pyrolysis*, 82 (2008) 170-177. <https://doi.org/10.1016/j.jaap.2008.03.007>.

[42] S. Zhang, F. Zhu, C. Bai, L. Wen, C. Zou, Thermal behavior and kinetics of the pyrolysis of the coal used in the COREX process, *Journal of Analytical and Applied Pyrolysis*, 104 (2013) 660-666. <https://doi.org/10.1016/j.jaap.2013.04.014>.

[43] M.M. Maroto-Valer, C.J. Atkinson, R.R. Willmers, C.E. Snape, Characterization of partially carbonized coals by solid-state C-13 NMR and optical microscopy, *Energy & Fuels*, 12 (1998) 833-842. <https://doi.org/10.1021/ef970196x>.

[44] S. Nomura, K.M. Thomas, Fundamental aspects of coal structural changes in the thermoplastic phase, *Fuel*, 77 (1998) 829-836. [https://doi.org/10.1016/s0016-2361\(97\)00259-7](https://doi.org/10.1016/s0016-2361(97)00259-7).

[45] S. Lee, J. Yu, M. Mahoney, P. Tremain, B. Moghtaderi, A. Tahmasebi, R. Stanger, T. Wall, J. Lucas, Study of chemical structure transition in the plastic layers sampled from a pilot-scale coke oven using a thermogravimetric analyzer coupled with Fourier transform infrared spectrometer, *Fuel*, 242 (2019) 277-286. <https://doi.org/10.1016/j.fuel.2019.01.024>.

- [46] Y. He, R. Zhao, L. Yan, Y. Bai, F. Li, The effect of low molecular weight compounds in coal on the formation of light aromatics during coal pyrolysis, *Journal of Analytical and Applied Pyrolysis*, 123 (2017) 49-55. <https://doi.org/10.1016/j.jaap.2016.12.030>.
- [47] A.H. Tchapda, V. Krishnamoorthy, Y.D. Yeboah, S.V. Pisupati, Analysis of tars formed during co-pyrolysis of coal and biomass at high temperature in carbon dioxide atmosphere, *Journal of Analytical and Applied Pyrolysis*, 128 (2017) 379-396. <https://doi.org/10.1016/j.jaap.2017.09.011>.
- [48] K. Miura, Mild conversion of coal for producing valuable chemicals, *Fuel Process. Technol.*, 62 (2000) 119-135. [https://doi.org/10.1016/s0378-3820\(99\)00123-x](https://doi.org/10.1016/s0378-3820(99)00123-x).
- [49] J. Yu, J.A. Lucas, T.F. Wall, Formation of the structure of chars during devolatilization of pulverized coal and its thermoproperties: A review, *Progress in Energy and Combustion Science*, 33 (2007) 135-170. <https://doi.org/10.1016/j.pecs.2006.07.003>.
- [50] K. I. S. M. T, *Structure and thermoplasticity of coal*, Nova publishers, 2005.